Environmental Science Advances

ROYAL SOCIETY OF CHEMISTRY

PAPER

View Article Online
View Journal | View Issue

Cite this: *Environ. Sci.: Adv.*, 2026, **5**, 543

Kinetic characteristics of heavy metals in soils in urban derelict contaminated lands

Yiming Sun, †[ab] Yanying Li, †[c] Qiuyu Rong,[d] Lan Wei [e] and Qingbao Gu*[a]

Despite being a hot topic for environmental management, heavy metal contamination in urban derelict industrial lands still lacks sufficient research into its kinetic parameters. This study aimed to systematically evaluate the contamination characteristics, labile fractions, lability, and solid-phase resupply kinetics of arsenic (As), cadmium (Cd), and lead (Pb) in various industrial soils using the Diffusive Gradients in Thin-films (DGT) technique and to elucidate the regulatory mechanisms of key soil physicochemical properties. The results indicated that the heavy metal pollution risk in the soils of different types of derelict industrial sites exhibited significant industry-specific differences. Non-ferrous metal smelting (NMS) and steel coking (SC) sites not only showed severe exceedances in total heavy metal concentrations but also displayed characteristics of high lability (high C_{DGT} and high R) and rapid kinetic release (low T_c and high R). These areas are classified as high potential risk zones requiring priority control. Specifically, the acidic environment at the SC2 site exacerbated the active release of Cd. In contrast, chemical industry (CI) and coal mining (CM) sites primarily faced As pollution risk, but their release kinetic processes were relatively slow. This research identified priority sites with high environmental risks from heavy metals and confirmed the unique advantage of the DGT technique for potential risk assessment. The findings provide a critical scientific basis for developing availability-based remediation and management strategies.

Received 24th September 2025
Accepted 17th December 2025

DOI: 10.1039/d5va00338e

rsc.li/esadvances

Environmental significance

This study addresses the critical environmental threat of toxic heavy metal (As, Cd, and Pb) contamination in industrial soils. By elucidating the dynamic behavior of these metals, the research establishes a scientific basis for developing more targeted and effective bioavailability-based remediation strategies. This is vital for mitigating the environmental risks associated with industrial pollution and for the sustainable management of contaminated lands.

1 Introduction

Heavy metal contamination has been one of the global problems of environmental management with the development of urbanization and industrialization.[1] Previous studies indicated that the toxicity of As, Pb and Cd has severely threatened human health.[2–4] For example, As can increase the risk of bladder cancer, lung cancer, skin cancer, and prostate cancer; Pb can damage the human central nervous system, leading to children's mental retardation, slow response, and shortened attention span; Cd mainly affects the reproductive health of women of childbearing age and children's health growth and development. Besides, heavy metal contamination has caused serious ecological problems as well, such as soil erosion, soil degradation and biodiversity reduction.[5] In order to optimize the urban industrial structure and layout, a large number of polluting enterprises have been moved out of the city center, leaving behind a large number of polluted sites. According to the statistics during 2001–2008, the number of closed and relocated industrial enterprises in China has reached more than 100 000 with a growth rate of 1984 per year.[6] Many studies have reported the contaminated cases from brownfield sites, for example, the Love Canal pollution incident in the United States.[7] Therefore, heavy metal contamination in urban derelict industrial lands has become a hot topic of environmental management and remediation.

Currently, traditional methods of risk assessments are based on the 'total concentration' of heavy metals in the soil obtained

[a]*State Key Laboratory of Environmental Criteria and Risk Assessment, Chinese Research Academy of Environmental Sciences, Beijing 100012, China. E-mail: guqb@craes.org.cn*

[b]*China CDC Key Laboratory of Environment and Population Health, National Institute of Environmental Health, Chinese Center for Disease Control and Prevention, Beijing 100021, China*

[c]*College of Environmental Science and Engineering, Dalian Maritime University, Dalian, Liaoning 116023, PR China*

[d]*Bureau of Hydrology and Water Resources, PRWRC of MWR, Guangzhou, 510610, China*

[e]*National Institute for Viral Disease Control and Prevention, Chinese Center for Disease Control and Prevention, Beijing 100021, China*

† Co-first authors: Yiming Sun; Yanying Li.

through exhaustive extractions, which assumes that they can be 100% absorbed by the human body, plants or other organism. However, these approaches often overestimate the availability of heavy metals, leading to resource waste and higher remediation costs. The availability of heavy metals is determined by their adsorption/desorption processes in soils. A distribution coefficient, K_d (the ratio of the amount of chemical adsorbed to the solid phase to that in the solution phase), is often used to characterized the interactions in solution and solid phases. Traditional approaches used for adsorption/desorption studies of heavy metals in soils only provide static data; they do not represent *in situ* conditions either. When organisms take up metals and reduce dissolved concentrations, metals that are readily desorbed from the solid phase can desorb to replenish the available pool. The dynamic sorption–desorption processes of heavy metals in soils can be characterized by the capacity (labile pool size) for re-mobilization and the rate of re-supply from the solid phase.

The diffusive gradients in thin-films (DGT) invented by Davison and Zhang in 1994 can effectively measure the available state of heavy metals *in situ* in soils.[8] A numerical model (DIFS, DGT-induced fluxes in soils and sediments) was developed to describe the dynamic processes between soil solution and solid phases. It has been successfully applied to further interpret the information obtained by DGT deployment.[8–10] Current research mainly focused on the application of DGT to heavy metal contaminated soils in agricultural lands and sediments by assessing human health risk through the indirect food chain (soil-plant-human body) approach,[8,9,11] and less research was conducted on industrial lands to evaluate the direct route (soil-human body) by oral uptake unintentionally entering the human body.[12] However, a recent study attempted to use DGT and DIFS models to assess the potential release risk of soil trace elements in different industrial lands and showed that DGT and DIFS models are an effective tool for assessing the potential release risk of trace heavy metal elements in urban soils.[13] This finding provides a good start for the feasibility of the DGT technique to determine the availability of heavy metals in the soils of industrial sites and provide valid information for risk assessment and remediation. However, the research only aimed at urban agricultural demonstration areas, urban residential areas, urban farmland downstream areas and urban green belts, not covering the types of derelict urban industrial soils. Urban derelict industrial lands have unique soil texture, properties and pollution levels, and the dynamic processes of heavy metals may differ from those in common urban soils and agricultural lands. Therefore, it is necessary to carry out relevant research in different industrial sites.

This study aimed to utilize DGT in urban derelict lands in North China to assess the potential release risk and dynamic characteristics of heavy metals in soils. North China has a long industrial history and large industrial area, with various industrial soil types. Five industrial types (chemical industry, coal mining, metal processing machinery manufacturing, non-ferrous metal smelting and steel coking) and three heavy metals (As, Pb, and Cd) were investigated in the study. We aimed to (1) investigate the pollution status of As, Pb and Cd in five types of derelict industrial sites; (2) assess the potential release risk of As, Pb and Cd in the five industrial types using *in situ* DGT and DIFS models.

2 Materials and methods

2.1 Sampling site description and sample treatment

The study area covered Heilongjiang, Jilin and Liaoning provinces in northern China. In total, 12 typical urban industrial contaminated sites (Fig. 1) involved in five industrial types (chemical industry (CI), coal mining (CM), metal processing machinery manufacturing (MPMM), non-ferrous metal smelting (NMS) and steel coking (SC)) were selected. In November 2020, a 40×40 m^2 grid was delineated in the center of each site and topsoil from 5 points (diagonal points of each grid) with a depth of 0–20 cm was collected from each site and mixed into one soil sample. A total of 12 soil samples were collected from 12 separate study sites. The sites denoted CI1–CI2, CI4 and CI5 were four chemical industry sites, located in the cities of Shenyang, Dandong and Dalian, respectively; CM1 and CM2 were two coal mining sites, located in the city of Shuangyashan; MPMM1 and MPMM3 were two metal processing machinery manufacturing sites, located in the cities of Harbin and Shenyang, respectively; NMS1 and NMS3 were two non-ferrous metal smelting sites, located in the city of Tonghua; SC2 and SC3 were two steel coking sites, located in the city of Changchun. All test soil samples were air-dried naturally at room temperature to remove stones, plant residues and other debris. After grinding, they were passed through a 2 mm sieve and stored in sealed bags. Table 1 shows the detailed information of the study sites and soil properties.

2.2 Determination of soil properties

0.5 g soil sample from each site was taken into a 50 mL test tube, added with 10 mL HNO_3 (14.5 mol L^{-1}) and 4 mL HF (22.5 mol L^{-1}), and digested for 12 hours. Subsequently, digestion was performed at 120 °C for 2 hours and 150 °C for 1 hour, and then the temperature was increased to 170 °C to evaporate the solution to 1 mL. The evaporated soil solution (1 mL) was diluted to 50 mL with ultrapure water and stored overnight. Then the suspension in the test tube was filtered with a 0.45 μm polyphenylene ether sulfone (PES) membrane. Finally, the total concentration of As, Pb, Cd, aluminium (Al), iron (Fe) and manganese (Mn) of all soil samples was determined by ICP-MS. Soil pH was measured using a pH meter. The method of Walkley and Black (1934) was used to determine the content of soil organic matter (SOM); the cation exchange capacity (CEC) was determined by the NAOAc-N-H_4OAc method.[14]

2.3 DGT measurements and soil solution extractions

The assembled Chelex 100-based and FeO DGT devices were used for DGT deployments. They were purchased from DGT Research Ltd (Lancaster, UK) with an exposure window of 2.54 cm^2. The configurations of the devices were described elswhere.[15,16] Two distinct types of DGT were employed: the Chelex

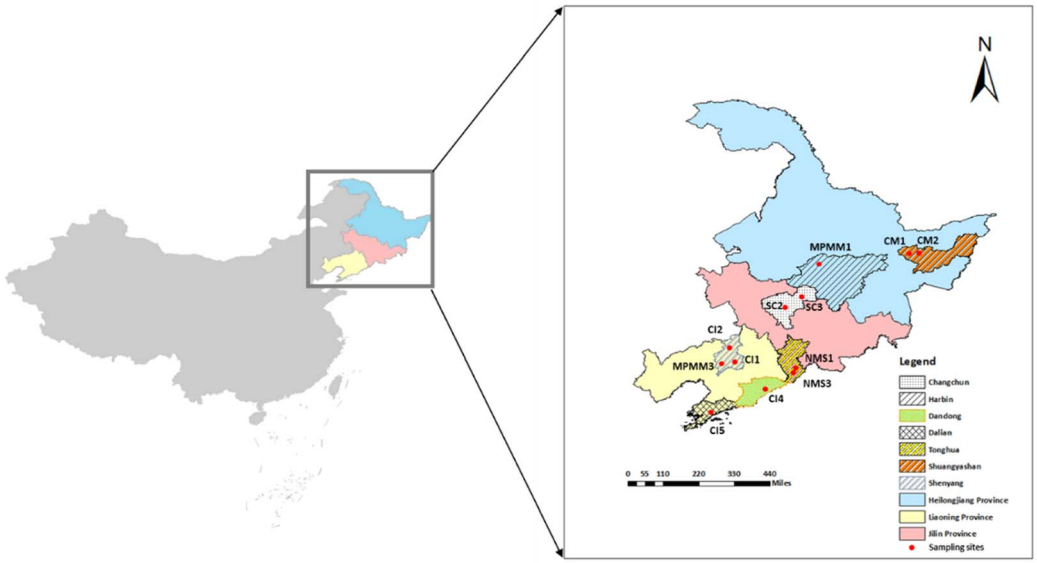

Fig. 1 Map of study area and sampling sites in this study.

100-based DGT was used for Pb and Cd, while the FeO-based DGT was used for As. 80 g soil was wetted with Milli Q water to 100% MWHC (maximum water holding capacity) and kept for 24 h for equilibrium. Then, the soil paste was placed into a plastic Petri dish, a layer of the paste was smeared onto the filter of the devices to ensure good contact and DGT devices were pressed into the soil paste. All the deployments were carried out in triplicate. After deployment for 24 h, the DGT devices were gently removed from the soil surface and immediately flushed with ultrapure water. Binding gels were removed and extracted according to the metal type: Chelex 100 binding gels (for Pb and Cd) were extracted with 1 mL 1 M HNO_3 for 24 h prior to measurements. FeO binding gels (for As) were extracted using 1 mL 1 M HNO_3 for 24 h to ensure complete desorption. The elution factors (f_{elute}) for As, Pb and Cd are all 0.8. After the deployments, soil paste was centrifuged for 20 min at a speed of 3500 rpm. The supernatant was acidized with HNO_3 and analyzed using ICP-MS after filtration with 0.45 μm syringe filters. For solid phase concentrations of Pb and Cd, samples of 2 g soil paste were taken and extracted with 20 mL 0.01 M $CaCl_2$ and shaken for 2 h. Another 2 g soil paste were shaken with 25 mL $NaHCO_3$ (adjusted to pH = 8.5) for 30 min to obtain solid phase concentrations of As. All the mixtures in the tubes were centrifuged at 3000 rpm for 10 min. The supernatant was filtered with 0.45 μm syringe filters and acidized with HNO_3 prior to analysis.

The concentrations of As, Pb and Cd determined using the DGT (C_{DGT}) were calculated using eqn (1).

Table 1 Soil properties of 12 industrial sites in this study[a]

Industrial type	Sample	pH	SOM	CEC	Total As (mg kg^{-1})	Total Pb (mg kg^{-1})	Total Cd (mg kg^{-1})	Total Al (mg kg^{-1})	Total Mn (mg kg^{-1})	Total Fe (mg kg^{-1})
Chemical industry (CI)	CI1	7.90	117	30.70	114.50*	125.20	1.40	44 705	1127	22 851
	CI2	10.35	84	27.90	54.10	87	2.48	65 913	871	32 434
	CI4	7.24	95.70	20.68	63.20*	86	0.38	39 765	345	28 578
	CI5	7.89	49.70	15.40	60.40*	37	0.21	36 981	756	42 283
Coal mining (CM)	CM1	6.75	85.30	21.15	69.20*	28.70	0.29	31 562	617	29 163
	CM2	7.52	216	12.20	48.30	53	0.26	51 762	335	22 148
Metal processing machinery manufacturing (MPMM)	MPMM1	7.23	86.35	15.90	60.70*	80.70	0.15	46 824	556	30 421
	MPMM3	7.64	41.10	19.10	50.60	28.10	0.38	17 704	338	18 739
Non-ferrous metal smelting (NMS)	NMS1	7.35	80.50	14.90	83.90*	107	0.76	70 439	518	32 080
	NMS3	7.25	95.15	17.00	167.87*	9606*	73.20*	50 497	1204	46 537
Steel coking (SC)	SC2	5.93	156	13.40	106.5*	3654*	24.30	58 759	779	35 568
	SC3	7.19	100	15.10	89.12*	521	1.33	68 855	773	35 343

[a] Note: the asterisk (*) indicates that the concentration of the metal exceeds the Soil Environmental Quality Standard. According to the Soil environmental quality: risk control standard for soil contamination of development land (GB36600-2018), the screening values for industrial land are 60 mg kg^{-1} for As, 800 mg kg^{-1} for Pb, and 65 mg kg^{-1} for Cd.

$$C_{DGT} = \frac{M\Delta g}{DAt} \quad (1)$$

where M is the amount of the analytes adsorbed on the binding layer (ng) and was calculated using the measured eluent concentration (C_{eluent}) as $M = C_{eluent} \times (V_{elute} + V_{gel})/f_{elute}$, where V_{elute} is the elution volume and f_{elute} is the elution factor; t is the deployment time (s); D is the diffusion coefficient of the analytes at 21.5 °C, with specific values of 4.89×10^{-6} for As, 5.54×10^{-6} for Cd, and 7.30×10^{-6} for Pb; A is the exposure area of the DGT device, with values of 2.54 cm^2 for Cd/Pb devices and 3.14 cm^2 for As devices; Δg is the total diffusional path length (0.094 cm).

2.4 Calculation of kinetic parameters and DIFS simulation

In this study, DIFS simulation was conducted to analyze the kinetic resupply of As, Pb and Cd in soil samples. The resupply index (R) was used for measuring the depletion of the soil solution concentration at the DGT-medium interface and represented the ability of the soil particles to resupply the analytes to soil solution.[17] The R values were calculated using eqn (2). There are three modes of resupply to the DGT devices determined using the R value. $R > 0.95$: rapid and sustained supply from the solid phase; $R < 0.1$: no resupply from the solid phase; the supply of the analytes is only by diffusion; $0.1 < R < 0.95$: an intermediate case; the analyte is partially resupplied.[18] The distribution coefficient (K_d), representing the equilibrium partitioning capability of the labile metal pool between the solid and liquid phases (eqn (3)), was calculated using the experimentally measured solid-phase labile concentration (C_{SE}) and soil solution concentration (C_{SS}). With R and K_d fixed as known experimental inputs, the response time (T_c) became the sole unknown variable. The 2D-DIFS model was configured with the standard DGT geometric parameters (Δg, A) and the diffusion coefficients (D) of the target metals. The model simulation was run by iteratively adjusting T_c until the simulated R value matched the experimentally observed R.

$$R = \frac{C_{DGT}}{C_{ss}} \quad (2)$$

where C_{DGT} refers to the time-integrated concentration measured by DGT. C_{ss} is the bulk concentration in soil solution.

$$K_d = \frac{C_{SE}}{C_{ss}} \quad (3)$$

Here, C_{SE} was determined *via* chemical extraction and C_{SS} was determined *via* centrifugation.

2.5 Quality assurance/quality control (QA/QC)

To ensure the accuracy, precision, and reliability of the chemical analysis, quality assurance/quality control procedures were strictly implemented including standard solution calibration, replicate measurements, recovery rate correction, application of calibration factors, and instrument calibration. All instruments used in the experiments were calibrated prior to each experiment. The calibration solutions were prepared using standard metal solutions of known concentrations to ensure the accuracy of the instrument response. Soil samples were uniformly mixed before sampling to ensure representativeness and homogeneity. The sample processing procedure involved standardized elution and DGT deployment conditions to minimize experimental errors. The recovery rate of the elution process was 85%, and therefore, a correction factor of 1.15 was applied to adjust the experimental results to account for potential losses during elution. Each sample was measured in triplicate, and the standard deviation and relative standard deviation of all measurements were within acceptable limits. Detection limits for ICP-MS were 0.05 μg L^{-1} for total As, total Pb, and total Cd, and 0.5 μg L^{-1} for total Al, total Fe, and total Mn. The analytical procedure followed HJ 700-2014, and the reported numerical precision was kept consistent with the detection limits.

2.6 Statistical analysis

All analyses were carried out and plots were obtained using the R 3.6.1 software. The Pearson correlation test was conducted to investigate the correlation between individual soil variables and the concentration/DGT labile of As, Pb and Cd. Significant differences in DGT-labile As, Pb and Cd among different industrial soil types were obtained using the Kruskal–Wallis rank sum test ($P < 0.05$).

3 Results and discussion

3.1 Physicochemical properties and total metal characteristics

The soils from the five investigated types of derelict industrial sites exhibited significant variations in physicochemical properties and varying degrees of heavy metal pollution characteristics (Table 1). Across the samples, soil pH ranged from 5.93 to 10.35, whilst the SOM varied between 41.10 and 216 g kg^{-1}. The CEC was in the range of 12.20 to 30.70 cmol kg^{-1}. These characteristics are broadly consistent with those reported for soils in the Northeast region.[19] Total concentrations of major elements also varied widely: Al from 17 704 to 70 439 mg kg^{-1}, Fe from 18 739 to 46 537 mg kg^{-1}, and Mn from 335 to 1204 mg kg^{-1}. The total concentrations of As, Pb, and Cd differed substantially amongst the study sites. The total As concentration was highest at site NMS3 (167.87 mg kg^{-1}) and lowest at site CM2 (48.30 mg kg^{-1}). The concentrations at the remaining sites decreased in the order of CI1 > SC2 > SC3 > NMS1 > CM1 > CI4 > MPMM1 > CI5 > CI2 > MPMM3. Similarly, the total Pb concentration was highest at NMS3 (9606 mg kg^{-1}) and lowest at MPMM3 (28.10 mg kg^{-1}), with the other sites ranking as follows: SC2 > SC3 > CI1 > NMS1 > CI2 > CI4 > MPMM1 > CM2 > CI5 > CM1. The highest total concentration of Cd was also found at NMS3 (73.20 mg kg^{-1}), whilst the lowest was recorded at MPMM1 (0.15 mg kg^{-1}). The order for the other sites was SC2 > CI2 > CI1 > SC3 > NMS1 > MPMM3 > CI4 > CM1 > CM2 > CI5.

According to the pollution assessment based on the screening values stipulated in the Soil environmental quality: risk control standard for soil contamination of development land (GB36600-2018) (the screening value As: 60 mg kg^{-1}, Pb: 800 mg kg^{-1}, and Cd: 65 mg kg^{-1}), the non-ferrous metal smelting (NMS) and steel coking (SC) sites were the most

severely contaminated. Notably, at sampling site NMS3, the concentration of Pb reached as high as 9606 mg kg^{-1} (exceeding the screening value by 12 times), while Cd and As concentrations reached 73.20 mg kg^{-1} (1.1-fold exceedance) and 167.87 mg kg^{-1} (2.8-fold exceedance), respectively, indicating a high potential risk of compound pollution. In the chemical industry (CI) and coal mining (CM) sites, As was identified as the predominant pollutant. For instance, As concentrations at sites CI1 and CM1 both exceeded the screening value of 60 mg kg^{-1}, whereas the exceedance levels for Pb and Cd were relatively minor. The metal processing machinery manufacturing (MPMM) sites exhibited relatively lower contamination levels, with only site MPMM1 showing a slight exceedance of As. Overall, based on the total concentration analysis, the degree of contamination followed the order NMS > SC > CI ≈ CM > MPMM.

3.2 DGT kinetic parameters of As, Pb and Cd from different industry types

The DGT-derived kinetic parameters for As, Cd, and Pb in the twelve soil samples from the CI sites, the CM sites, the MPMM sites, the NMS sites and the SC sites are presented in Table 2. The DGT-measured labile concentrations (C_{DGT}), along with the solution (C_{SS}) and solid-phase labile (C_{SE}) fractions, provide more direct information on environmental behaviour than total concentrations alone.[20,21]

Table 2 C_{DGT}, C_{SS}, C_{SE}, K_d and T_c of As, Cd and Pb at the 12 industrial sites[a]

Industrial type	Sample	Metal	C_{DGT} (mean ± SD, ng mL^{-1})	C_{SS} (ng mL^{-1})	C_{SE} (mean ± SD, ng g^{-1})	R	T_c (s)	K_d (mL g^{-1})	Potential risk
Chemical industry (CI)	CI1	As	6.56 ± 0.21	30.36	1185.70 ± 120.55	0.22	1.77×10^4	39.06	Low
	CI2	As	1.44 ± 0.31	28.72	784.84 ± 3.40	0.05	1×10^7	27.32	Low
	CI4	As	1.33 ± 0.08	9.54	134.00 ± 48.25	0.13	1.75×10^5	14.04	Low
	CI5	As	0.01 ± 0.01	0.71	90.95 ± 36.73	0.01	1×10^7	129.08	Low
	CI1	Cd	0.03 ± 0.01	4.38	1.42 ± 0.79	0.01	53.55	0.32	High
	CI2	Cd	0.02 ± 0.01	0.80	1.46 ± 0.46	0.02	1×10^7	1.84	Low
	CI4	Cd	0.05 ± 0.01	0.42	8.91 ± 8.50	0.11	0.87×10^5	21.27	Low
	CI5	Cd	0.02 ± 0.001	0.33	0.15 ± 0.20	0.05	1×10^7	0.45	Low
	CI1	Pb	0.32 ± 0.47	380.70	23.98 ± 5.12	0.01	111.40	0.06	High
	CI2	Pb	0.16 ± 0.13	5.59	24.22 ± 6.25	0.03	1×10^7	4.33	Low
	CI4	Pb	0.34 ± 0.13	19.93	206.75 ± 285.82	0.02	1×10^7	10.37	Low
	CI5	Pb	0.06 ± 0.07	6.33	6.08 ± 2.55	0.01	1×10^7	0.96	Low
Coal mining (CM)	CM1	As	0.51 ± 0.01	0.88	126.00 ± 7.02	0.58	272.30	143.23	High
	CM2	As	0.07 ± 0.01	11.19	55.13 ± 0.93	0.01	1×10^7	4.92	Low
	CM1	Cd	0.06 ± 0.02	0.45	5.38 ± 4.11	0.14	1.32	11.89	High
	CM2	Cd	0.04 ± 0.003	0.36	0.98 ± 0.31	0.10	0.34×10^5	2.77	Low
	CM1	Pb	0.10 ± 0.06	3.04	20.65 ± 7.89	0.03	1×10^7	6.79	Low
	CM2	Pb	0.12 ± 0.12	3.56	10.64 ± 2.60	0.03	1×10^7	2.99	Low
Metal processing machinery manufacturing (MPMM3)	MPMM1	As	0.30 ± 0.03	2.20	79.34 ± 19.91	0.14	0.85×10^5	36.05	Low
	MPMM3	As	0.16 ± 0.02	1.10	141.34 ± 16.33	0.13	1.92×10^5	128.71	Low
	MPMM1	Cd	0.03 ± 0.004	0.62	0.78 ± 0.76	0.05	1×10^7	1.27	Low
	MPMM3	Cd	0.05 ± 0.01	0.57	3.48 ± 3.16	0.09	1×10^7	6.15	Low
	MPMM1	Pb	0.21 ± 0.21	42.32	23.77 ± 31.30	0.01	13.20	0.56	High
	MPMM3	Pb	0.01 ± 0.05	2.72	196.09 ± 225.40	0.01	1×10^7	72.24	Low
Non-ferrous metal smelting (NMS)	NMS1	As	1.41 ± 0.03	6.21	253.15 ± 13.09	0.23	1.55×10^4	40.77	Low
	NMS3	As	1.84 ± 0.13	12.41	2891.55 ± 90.31	0.15	0.83×10^5	233.07	Low
	NMS1	Cd	0.16 ± 0.02	0.96	3.46 ± 21.75	0.17	0.16	3.62	High
	NMS3	Cd	22.37 ± 0.47	17.21	377.94 ± 23.25		0.02	21.96	High
	NMS1	Pb	0.39 ± 0.12	7.64	94.66 ± 21.75	0.05	1×10^7	12.39	Low
	NMS3	Pb	30.13 ± 3.18	57.32	132.27 ± 15.63	0.53	1.59	2.31	High
Steel coking (SC)	SC2	As	0.96 ± 0.17	6.15	1354.05 ± 79.90	0.16	0.63×10^5	220.31	Low
	SC3	As	0.14 ± 0.05	6.14	660.02 ± 25.00	0.02	1×10^7	107.45	Low
	SC2	Cd	24.82 ± 1.50	18.16	1039.10 ± 26.10		1.20	57.21	High
	SC3	Cd	0.23 ± 0.02	0.42	2.60 ± 0.02	0.54	0.21	6.15	High
	SC2	Pb	25.01 ± 0.36	308.73	542.75 ± 20.10	0.08	1×10^7	1.76	Low
	SC3	Pb	1.22 ± 0.31	8.80	9.91 ± 0.63	0.14	0.04	1.13	High

[a] Note: potential environmental risk of contaminants (As, Pb, and Cd) in the soils was assessed based on the comprehensive interpretation of different DGT parameters (R, T_c, and K_d). Risk levels were determined by evaluating the combined effect of K_d, T_c, and R at the solid–liquid interface. High-risk conditions are characterized by rapid kinetics and high dynamic exchange, promoting contaminant mobilization and availability. Specifically, the following criteria guided the assessment: low T_c (typically < 10^3 s) indicates a fast kinetic response where the solid phase can rapidly replenish the pore water concentration. High R (approaching 1) signifies strong dynamic lability and minimal solid-phase limitation on flux. Sites exhibiting both low T_c and high R were classified as having a high potential release risk, regardless of the K_d value, as the entire contaminant pool is rapidly exchangeable. Conversely, high T_c (typically > 10^5 s) and low R (approaching 0) indicate that contaminants are stably immobilized and kinetically controlled by slow release mechanisms, resulting in a low potential release risk.

3.2.1 Chemical industry sites. For As, the values of C_{DGT}, C_{SS}, and C_{SE} followed a consistent trend across the four samples: CI1 > CI2 > CI4 > CI5. The distribution coefficient (K_d) ranged from 14.04 to 39.06 mL g^{-1}, with the highest value observed at site CI5, followed by CI1, CI2, and CI4. The R value ranged from 0.05 to 0.22, with the highest value at CI1, decreasing in the order of CI4 > CI2 > CI5. The response time (T_c) exceeded 10^3 s for all four samples. The consistent trends for the DGT concentration parameters suggest that the As contamination sources and speciation were similar across these sites. The results indicate that site CI5 possessed the strongest As sorption capacity, whilst As lability was greatest in sample CI1. The uniformly high T_c values suggest that the resupply of As from the solid phase was slow, implying that As was relatively stable in these soils. For Cd, C_{DGT} and C_{SE} showed a similar trend, being highest at CI4 and lowest at CI5. This differed from the trend for C_{SS}, which was highest at CI1. The K_d values ranged from 0.32 to 21.27 mL g^{-1}, with the maximum at CI4 and the minimum at CI1. R values ranged from 0.006 to 0.11, with the highest at CI4 and lowest at CI1. The T_c was lowest at CI1, whilst it exceeded 10^3 s in the other samples. The high C_{SS} at CI1 indicates its greatest water-solubility and lability, reflecting a higher environmental risk. Site CI4 had the strongest sorption capacity (highest K_d), whereas CI1 had the weakest. Correspondingly, the resupply rate for Cd was fastest at site CI1. For Pb, C_{DGT} and C_{SE} followed a consistent trend (CI4 > CI1 > CI2 > CI5), which differed from that of C_{SS} (highest at CI1). K_d values ranged from 0.06 to 10.37 mL g^{-1}, being highest at CI4 and lowest at CI1. R values ranged from 0.001 to 0.03, with the maximum at CI2 and the minimum at CI1. The T_c was lowest at CI1 and exceeded 10^3 s in the other samples. The high C_{SS} value at CI1 suggests the greatest water-solubility and lability of Pb, implying a higher environmental risk. Site CI4 showed the strongest sorption capacity, and CI1 showed the weakest. Pb lability was greatest at site CI2 (highest R value), while the resupply rate was fastest at CI1 (lowest T_c). In summary, although the trends for C_{DGT} and C_{SE} were broadly consistent, the variations in K_d, R value, and C_{SS} reveal distinct behavioural characteristics for As, Pb, and Cd in these soils. Site CI4 generally exhibited a higher sorption capacity. In contrast, site CI1 was consistently characterised by the greatest heavy metal lability and the fastest resupply rates, indicating that the availability and environmental risks of Pb and Cd are particularly high in this soil.

3.2.2 Coal mining sites. In the two soil samples from the CM sites, for As, the trends for C_{DGT} and C_{SE} were consistent (CM2 > CM1), but this was opposite to the trend for C_{SS} (CM1 > CM2). The K_d value was significantly higher at CM1 (143.23 mL g^{-1}) than at CM2 (4.92 mL g^{-1}), indicating a stronger sorption capacity. However, the R value was also substantially higher at CM1 (0.58 *vs.* 0.01 at CM2), suggesting greater As lability. The higher C_{SS} at CM1 further supports this observation of greater lability, reflecting a higher concentration of As in the soil solution. The T_c value was 272.30 s at CM1, whilst at CM2 it exceeded 10^3 s. For Cd, the parameters C_{DGT}, C_{SS}, and C_{SE} all followed a consistent trend (CM1 > CM2). The K_d value was higher at CM1 (11.89 mL g^{-1}) than at CM2 (2.77 mL g^{-1}). Similarly, the R value was greater at CM1 (0.14) compared to CM2 (0.10). The T_c value at CM1 was only 1.32 s, whereas it was greater than 10^3 s at CM2. This indicates that at site CM1, Cd exhibited not only a higher sorption capacity and concentration but also greater lability and a much faster resupply rate. For Pb, C_{DGT} and C_{SS} followed the same trend (CM2 > CM1), which was contrary to the trend for C_{SE} (CM1 > CM2). The sorption capacity was stronger at CM1, with a K_d of 6.79 mL g^{-1} compared to 2.99 mL g^{-1} at CM2. However, lability (both R values were 0.03) and the resupply rate (both T_c values > 10^3 s) showed no significant difference between the two sites. Although the extractable solid-phase concentration (C_{SE}) was higher at CM1, the solution concentration (C_{SS}) was higher at CM2, indicating relatively complex behaviour for Pb. In summary, the combination of high sorption capacity and high lability for As at site CM1 poses a considerable environmental risk, particularly during environmental disturbances. The higher water-solubility and much faster resupply rate of Cd at CM1 also signify an elevated risk. For Pb, the environmental risk may not differ significantly between the two sites, given their comparable lability and slow resupply rates. Nevertheless, the higher solution concentration (C_{SS}) of Pb at site CM2 indicates potential for environmental transfer. Overall, site CM1 is considered to present a greater risk, primarily due to the behaviour of As and Cd.

3.2.3 Metal processing machinery manufacturing sites. In the two soil samples from the MPMM sites, for As, C_{DGT} and C_{SS} followed a consistent trend (MPMM1 > MPMM3), which was opposite to the trend for C_{SE} (MPMM3 > MPMM1). The sorption capacity for As was considerably stronger at site MPMM3 (K_d = 128.71 mL g^{-1}) than at MPMM1 (K_d = 36.05 mL g^{-1}). The lability, as indicated by the R value, was slightly higher at MPMM1 (0.14) compared to MPMM3 (0.13). The response time (T_c) exceeded 10^3 s for both samples, indicating a low resupply rate. For Cd, the trends for C_{DGT} and C_{SE} were consistent (MPMM3 > MPMM1), but opposite to the trend for C_{SS} (MPMM1 > MPMM3). The sorption capacity was stronger at MPMM3 (K_d = 6.15 mL g^{-1}) than at MPMM1 (K_d = 1.27 mL g^{-1}), suggesting greater immobilisation. However, the R value was also higher at MPMM3 (0.09) than at MPMM1 (0.05), indicating slightly higher lability for Cd at this site. The T_c for both samples exceeded 10^3 s. For Pb, C_{DGT} and C_{SS} followed the same trend (MPMM1 > MPMM3), which was contrary to the trend for C_{SE} (MPMM3 > MPMM1). Site MPMM3 had a much stronger sorption capacity (K_d = 72.24 mL g^{-1}) compared to MPMM1 (K_d = 0.56 mL g^{-1}). The R values for both sites were identical (0.05). The resupply rate at MPMM1 was fast (T_c = 13.20 s), whereas the high T_c value (>10^3 s) at MPMM3 indicates that Pb was not readily resupplied from the solid phase in this soil. In summary, for As, the higher solubility and lability at site MPMM1 suggest that it may pose a greater ecological risk than MPMM3. For Cd, both the sorption capacity and lability were higher at MPMM3, indicating a higher potential availability and an environmental risk that warrants attention. For Pb, despite the much stronger sorption capacity at MPMM3, the significantly faster resupply rate at MPMM1 suggests a potential environmental risk, as Pb could be

released from this soil under changing conditions such as precipitation.

3.2.4 Non-ferrous metal smelting sites. In the two soil samples from the NMS sites, for As, the values of C_{DGT}, C_{SS}, and C_{SE} followed a consistent trend across the two sites (NMS3 > NMS1). The sorption capacity (K_d) was significantly stronger at NMS3 (233.07 mL g^{-1}) than at NMS1 (40.77 mL g^{-1}), suggesting that As was less mobile at this site. Conversely, the lability of As, indicated by the R value, was slightly higher at NMS1 (0.23) compared to NMS3 (0.15), implying a greater environmental risk from As at NMS1. The response time (T_c) for both samples exceeded 10^3 s. The DGT concentration parameters for Cd also followed a consistent trend (NMS3 > NMS1). The sorption capacity for Cd was stronger at NMS3 (K_d = 21.93 mL g^{-1}) than at NMS1 (K_d = 3.62 mL g^{-1}). The resupply rate was much slower at NMS1 (T_c > 0.16 s), whereas the significantly faster rate at NMS3 (T_c = 0.02 s) shows that Cd was readily resupplied in this soil. For Pb, the DGT concentration parameters consistently showed higher values at NMS3 than at NMS1. However, the sorption capacity was weaker at NMS3 (K_d = 2.31 mL g^{-1}) compared to NMS1 (K_d = 12.38 mL g^{-1}). Conversely, the lability of Pb was much greater at NMS3 (R value = 0.53) than at NMS1 (R value = 0.05), indicating a larger environmental risk from Pb at site NMS3. The T_c value at NMS3 was > 10^3 s. At NMS1, although the sorption capacity was stronger and lability was lower, the resupply rate was also relatively high (T_c > 1.59 s).

3.2.5 Steel coking sites. In the two soil samples from the steel coking (SC) sites, for As, the values of C_{DGT}, C_{SS}, and C_{SE} followed a consistent trend (SC2 > SC3). The sorption capacity (K_d) was significantly stronger at SC2 (220.31 mL g^{-1}) than at SC3 (107.45 mL g^{-1}), suggesting that As was less mobile in the SC2 soil. Although lability was slightly higher at SC2 (R value of 0.16 *vs.* 0.02 at SC3), the overall environmental risk was considered relatively low, as the response time (T_c) for both samples exceeded 10^3 s. The DGT concentration parameters for Cd also followed a consistent trend (SC2 > SC3). The sorption capacity (K_d of 57.21 *vs.* 6.15 mL g^{-1}) of Cd was significantly higher at SC2 than at SC3. Although Cd was more readily adsorbed at SC2, its high lability indicates that its environmental risk warrants attention. The very rapid resupply rate at SC3 (T_c = 0.21 s), alongside the fast rate at SC2 (T_c = 1.23 s), means both sites pose a considerable environmental risk that requires special attention. For Pb, the DGT concentration parameters were consistently higher at SC2 than at SC3. The sorption capacity for Pb was slightly stronger at SC2 (K_d = 1.76 mL g^{-1}) than at SC3 (K_d = 1.13 mL g^{-1}). However, lability was lower at SC2 (R value = 0.08) compared to SC3 (R value = 0.14). Furthermore, the resupply rate was much slower at SC2 (T_c > 10^3 s) than at SC3, where it was extremely fast (T_c = 0.04 s). Consequently, the environmental risk from Pb was smaller at SC2, whilst the higher lability and rapid resupply at SC3 indicate a greater environmental risk. In summary, the environmental risk from As was considered low at both steel coking sites. In contrast, Cd at both locations poses a significant risk requiring attention and control: site SC2 due to its high lability and fast resupply, and site SC3 due to its extremely rapid resupply rate. The risk from Pb was relatively low at SC2 owing to its stronger sorption capacity and lower mobility. However, the environmental risk from Pb was considerably higher at SC3 because of its greater lability and very fast resupply rate, indicating that this site also requires the implementation of control measures.

3.3 Potential risk assessment based on DGT measurement and DIFS

3.3.1 Labile concentration measured by DGT. The DGT-labile concentration (C_{DGT}) reflects the lability of heavy metals in soil pore water. As shown in Fig. 2A, the lability varies significantly across the different industrial types. The steel coking (SC) and non-ferrous metal smelting (NMS) sites exhibited extremely high availability. The average C_{DGT} of Cd at SC sites was approximately 12.52 ng mL^{-1}, and the average C_{DGT} of Pb at NMS sites reached a high value of 15.26 ng mL^{-1}, values which were significantly higher than those found at the other three types of sites. As showed the highest average availability at the chemical industry (CI) sites (2.33 ng mL^{-1}), followed by NMS sites (1.63 ng mL^{-1}). This suggests that although the total As concentration at CI sites may be lower than that at NMS sites, its chemical speciation is likely more labile.

This study investigated the heavy metal contamination status and DGT kinetic characteristics of 12 soil samples affected by industrial activities (Table 2). Specifically at the sampling point level, the risk identified by DGT did not completely align with the total concentration analysis. At the non-ferrous metal smelting (NMS3) site, the C_{DGT} of Cd reached 22.37 ng mL^{-1} and Pb reached 30.13 ng mL^{-1}, leading to its classification as "high potential risk". Furthermore, at the steel coking (SC2) site, despite the acidic soil conditions, the availability of Cd was exceptionally high (C_{DGT} 24.82 ng mL^{-1}), even surpassing that of NMS3, which had a higher total Cd concentration. This finding demonstrates the extremely strong potential risk posed by Cd at SC2. Conversely, the total Pb concentration at the metal processing (MPMM1) site (80.70 mg kg^{-1}) was far below the control standard (800 mg kg^{-1}). Nevertheless, this sample was flagged as "high potential risk," suggesting that Pb at this site exists predominantly in an extremely readily labile form.

3.3.2 Lability and availability and resupply dynamics. The different DGT parameters (R, T_c, and K_d) reveal the intrinsic mechanism of heavy metal release from different industrial pollution sources (Fig. 2B–D). The R value, which reflects the ability of the soil solid phase to replenish heavy metals to the pore water, is a key indicator for assessing both the short-term and long-term lability and availability of heavy metals. A high R value indicates that the solid phase can effectively buffer the concentration in the pore water. This implies that under conditions of continuous depletion (*e.g.*, *via* plant uptake or leaching), the soil can sustain the release of heavy metals, thereby maintaining high availability and environmental exposure risk.[22,23] At the specific sampling sites (Table 2), the R values for As in most soil samples ranged between 0.10 and 0.58, indicating a moderate resupply ability from the solid phase across the sites. However, the CM1 site exhibited the

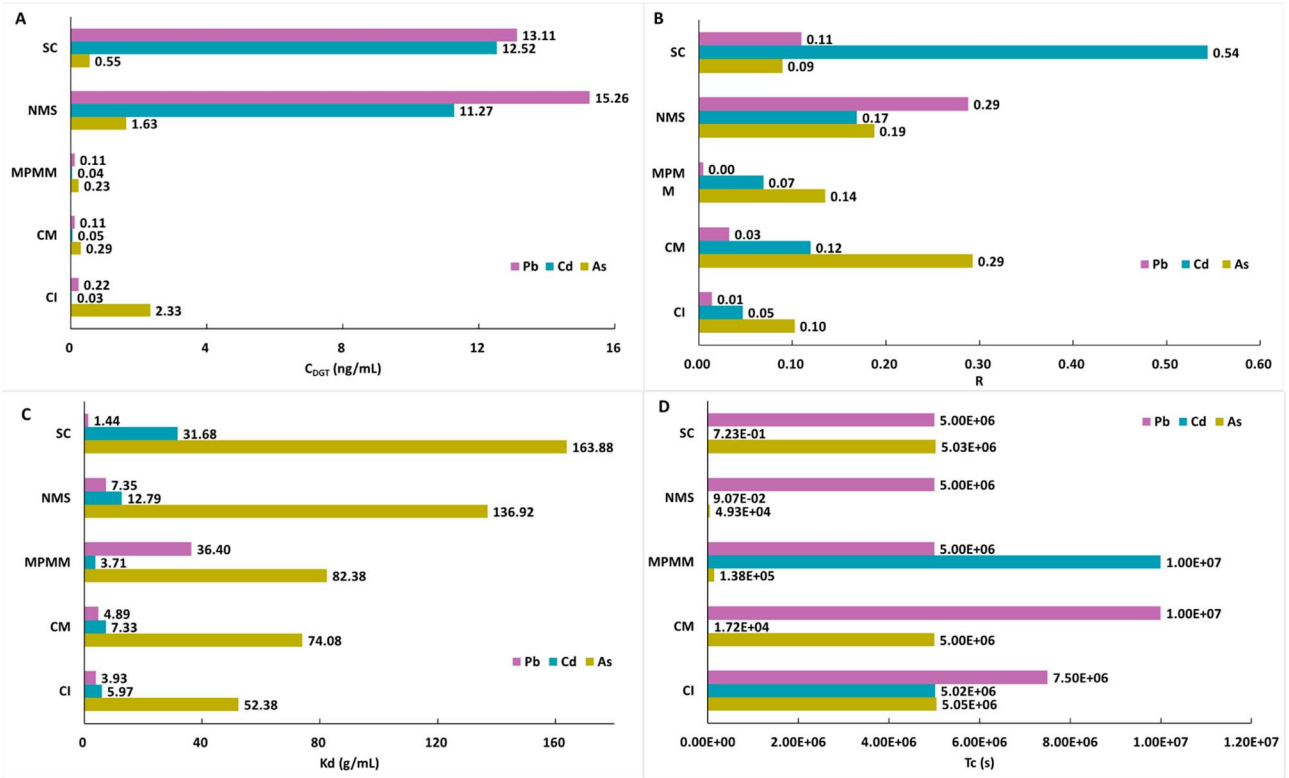

Fig. 2 DGT measured concentrations (A), R values (B), K_d (C) and T_c (D) of As, Cd and Pb in different industrial types. The values of C_{DGT}, K_d, R, and T_c are calculated based on the average values of samples from different industrial types.

highest dynamic response ($R = 0.58$) among all samples. For Cd, the R values at sites SC2 and NMS3 were greater than 0.95, demonstrating a very strong solid-phase resupply ability. This signifies that Cd at these two sites has extremely high potential availability and migration risk. In contrast, the R values for the chemical plant samples were low (<0.1), indicating limited resupply ability. The R values for Pb in most samples were less than 0.1, suggesting that Pb was predominantly present in an immobilised state. The relatively higher R values for Pb at NMS3 and SC3 indicate that Pb still possessed a degree of lability at these specific sites. From the perspective of industrial type (Fig. 2B), Cd at the steel coking (SC) sites exhibited the highest average R value (0.54). This implies that when Cd in the pore water is depleted, the solid phase can rapidly resupply it, maintaining the solution concentration at a relatively high level (C_{DGT} is approximately 0.54 times that of C_{SS}). The R value for Pb at the non-ferrous metal smelting (NMS) sites was the second highest (0.29), similarly indicating a strong sustained release capacity. Conversely, the R values at the chemical (CI) and metal processing (MPMM) sites were extremely low (<0.10). This suggests that heavy metal release in these sites is primarily controlled by diffusion, with limited solid-phase resupply capacity, making them prone to localized depletion zones.

The distribution coefficient (K_d) reflects the partitioning preference of heavy metals between the solid and liquid phases and the overall sorption strength of the solid matrix. The response time (T_c), in turn, reflects the rate of the kinetic processes of desorption from the solid phase; that is, the rate of resupply to the soil solution. Focusing on the specific sampling sites (Table 2), the K_d values for As varied over a wide range (4.9–233.07 mL g^{-1}), with sites such as NMS3, SC2, and CM1 showing strong sorption capacities. The T_c values for most As samples were high ($T_c > 10^3$), indicating that the solid-phase resupply of As was generally slow and that As tended to be stably immobilised in the soil. Notably, the T_c at site CM1 was significantly lower at 272.30 s, suggesting the fastest solid-phase kinetic response in this location. For Cd, K_d values ranged between 0.01 and 64 mL g^{-1}. The T_c values varied considerably; samples from sites CI1, CM1, SC2, SC3, NMS1, and NMS3 had T_c values of less than 100 s. This indicates that Cd has a fast resupply rate in these soils and is thus prone to migration and dissolution. For most Pb samples, the K_d values were moderate, although site MPMM3 exhibited a strong sorption capacity (K_d = 72.24 mL g^{-1}). The T_c values differed greatly. Sites SC3, NMS3, and MPMM1 had T_c values of less than 100 s, showing that the resupply of Pb was very fast in these soils, whereas in the other samples, Pb appeared to be almost immobile. From the perspective of industrial type (Fig. 2C and D), As at the steel coking (SC) sites exhibited a very high mean K_d value (163.88 g mL^{-1}). This suggests that a large amount of As is strongly adsorbed and immobilized in the solid phase, making it difficult to migrate into the liquid phase. This finding explains why, despite having high total As concentrations, the risk at SC sites is relatively controllable. In terms of characteristic time (T_c), a smaller T_c value

indicates faster solid-phase desorption. Cd at NMS3 (T_c = 0.02 s) and Pb at SC3 (T_c = 0.04 s) showed millisecond-level response times. This suggests that heavy metals in these soils are extremely loosely bound, posing an extreme environmental risk. Conversely, the T_c values for the vast majority of low-risk sites (*e.g.*, Pb at CI5, CM2, and SC2) were all 1×10^7 s, indicating that their heavy metals are firmly locked within crystal lattices or on difficult-to-desorb sites, resulting in hindered release kinetics.

3.4 Correlation between soil physicochemical properties and different DGT measurements

Soil physicochemical properties have a critical influence on the speciation, adsorption–desorption behaviour, and lability of heavy metals.[24,25] The correlation analysis in this study provides direct evidence of the mechanisms by which these properties control the speciation and dynamic behaviour of As, Cd, and Pb. Correlation analysis between the different DGT parameters (C_{DGT}, C_{SS}, C_{SE}, R, T_c, and K_d) and soil physicochemical properties (pH, SOM, CEC, total Al, total Mn, and total Fe) revealed several key relationships (Fig. 3).

For As, the strong correlation (r = 0.93) between total As and C_{SE} indicates that the C_{SE} pool serves as a major control on the overall As content in the soil. This tight coupling indicates that a significant fraction of the total As is readily available for dynamic exchange or exists in a potentially bioavailable/readily extractable form. This may be due to the presence of multiple As species (*e.g.*, As(III) and As(V)), which exhibit different sorption/desorption characteristics under specific pH and redox conditions. The significant positive correlation (r = 0.69) between C_{DGT} and CEC suggests that the cation exchange capacity has an important influence on the availability of labile As, possibly by indirectly affecting the sorption and diffusion of As through its effects on the ionic strength of the soil solution and the surface charge of soil particles. The positive correlations of total As with total Mn (r = 0.79) and total Fe (r = 0.55) confirm the important role of Fe–Mn oxides in the immobilisation of As,[26] whose surfaces possess abundant hydroxyl functional groups capable of binding arsenate or arsenite. The positive correlation (r = 0.61) between K_d and C_{SE} suggests a link between sorption capacity and availability; a stronger sorption capacity might imply more stable binding, yet a portion of this sorbed fraction may simultaneously exist in a dynamic, DGT-labile state.

For Cd, the strong positive correlations (r > 0.8) of total Cd with Cd_C_{DGT}, Cd_C_{SS}, and the R value, along with the strong positive correlations (r > 0.89) among its various labile fractions, indicate that Cd is highly labile and mobile in these soils, with rapid and highly correlated transformations between its different available forms. This is likely related to Cd existing predominantly as free ions or weakly complexed species and its relatively weak competitive ability for soil sorption sites. While the positive correlations of total Cd with total Mn (r = 0.60) and total Fe (r = 0.64) indicate that Fe–Mn oxides also contribute to Cd immobilisation, their sorption strength for Cd may be relatively weaker than that for Pb.[27,28] The negative correlation (r = −0.50) between pH and Cd_C_{SE} clearly shows that acidic conditions significantly increase the availability of Cd, as H^+ ions compete with Cd^{2+} for sorption sites and promote the desorption of Cd from the solid phase.

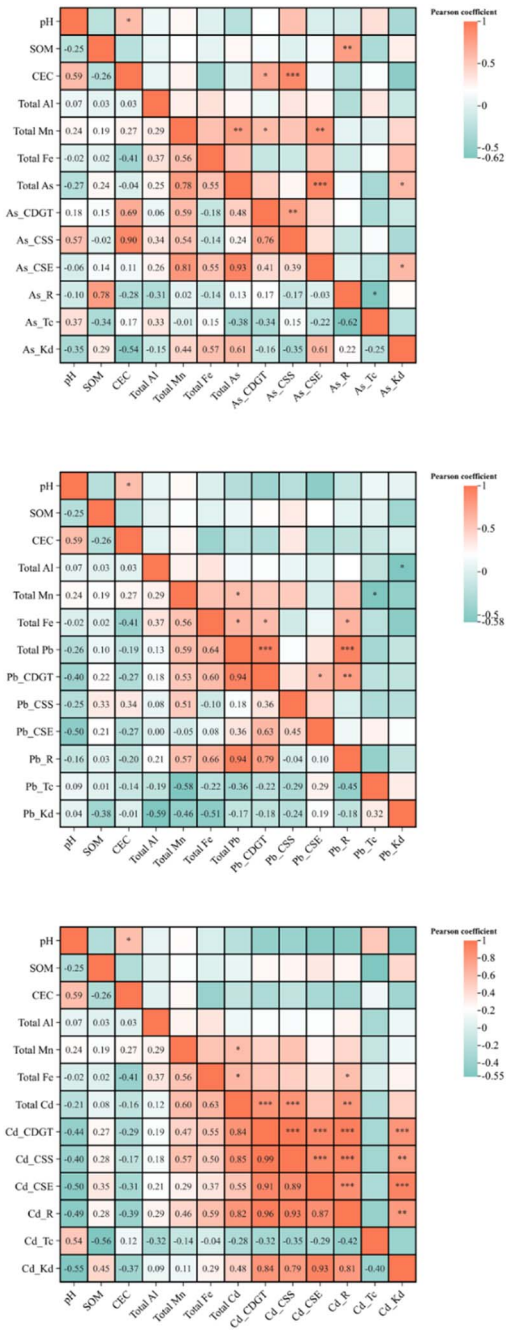

Fig. 3 Correlation between soil physicochemical properties and various measurements (C_{DGT}, R, T_c, K_d, C_{SS}, and C_{SE}) of As (top), Pb (middle) and Cd (bottom) in soils.

For Pb, the strong positive correlations of total Fe (r = 0.64) and total Mn (r = 0.59) with total Pb provide powerful evidence that Fe–Mn oxides play a crucial role in the immobilisation of Pb. These oxides strongly fixate Pb *via* adsorption, co-precipitation, or surface complexation. At the same time, a strong correlation (r = 0.60) was also found between total Fe and Pb_C_{DGT}. This indicates that although Fe oxides immobilise Pb, the surface-adsorbed Pb may, under certain

conditions, remain in a DGT-labile state, or that the dynamic transformation of these oxides (*e.g.*, through redox cycling) could influence the release of Pb. The moderate negative correlation ($r = -0.50$) between pH and Pb_C_{SE} again highlights the increased availability of Pb under acidic conditions. Finally, the negative correlations of Pb_T_c with total Mn ($r = -0.58$) and the R value ($r = -0.45$) indicate that a higher manganese content and a more sustained resupply are associated with a faster resupply rate (a lower T_c), highlighting the dynamic role of manganese oxides in controlling the release kinetics of Pb.

3.5 Assessment of potential environmental risk

The risk associated with heavy metal contamination depends not only on the total concentration but more critically on lability and resupply potential in the environment. The DGT measurements and DIFS modelling offer a more comprehensive perspective for evaluating potential ecological and human health risks.[29,30] By integrating the labile concentration (C_{DGT}), the solid-phase resupply ability (R value), and the resupply rate (T_c), alongside the controlling influence of soil physicochemical properties, we can identify sites where heavy metals exhibit high activity and pose a potential environmental risk including CI1 (Cd, Pb), CM1 (As, Cd), NMS1/NMS3 (Cd, Pb), MPMM1 (Pb) and SC2/SC3 (Cd, Pb) (Table 2). The primary characteristics of these sites are that the heavy metals may not only exhibit high total concentrations, but, more importantly, their kinetic release is extremely rapid (T_c is short and R is relatively high). This rapid release enables the sustained flux of toxic metals into the soil solution, making these sites a priority target for environmental remediation and control.

At the chemical industry site CI1, Pb (T_c = 111.40 s, K_d = 0.06) and Cd (T_c = 53.55 s, K_d = 0.32) displayed the greatest lability and fastest resupply rates. Despite not having the highest total concentrations, the high lability and rapid resupply characteristics of these metals confer a higher potential environmental risk at this site than at the others. At the coal mining site CM1, As exhibited both high sorption capacity (high K_d) and high resupply ability ($0.1 < R < 0.95$). Combined with its high solution concentration (C_{SS}), this suggests a high potential risk of release under environmental disturbances. Cd at this site also poses a significant potential environmental risk due to its high solubility, high lability, and very fast resupply rate. At the non-ferrous metal smelting site NMS3, Pb and Cd presented high labile concentrations and extremely fast resupply rates, identifying this as the area of the highest overall risk. At the steel coking sites SC2 and SC3, Cd requires special attention due to its high lability and fast resupply rate. The risk from Pb at SC3 was also high for the same reasons. Furthermore, the moderate negative correlation ($r = -0.50$) between pH and the bioavailable Cd fraction (Cd_C_{SE} = 1039 ± 26.10 in SC2) underscores that acidic conditions (low pH = 5.93 in SC2) significantly increase the availability of Pb. Therefore, in contaminated sites with low pH, caution should be exercised regarding the high ecological risk from Pb, even if its total concentration is not exceptionally high.[31]

3.6 Environmental implications and management recommendations

The heavy metal DGT kinetic characteristics and the correlations with soil properties revealed in this study have significant implications for the potential risk assessment and management of Pb, Cd, and As contamination. Given the significant influence of pH on the availability of Cd and Pb, adjusting the soil pH to neutral or weakly alkaline conditions is an effective measure for reducing their lability and availability at acidic contaminated sites. This can be achieved through the application of liming agents such as lime or carbonates.[32–34] The demonstrated role of Fe–Mn oxides in the immobilisation of As, Cd, and Pb makes them important potential remediation materials. The application of Fe–Mn oxides or their precursors could be considered at contaminated sites to promote the adsorptive immobilisation of heavy metals, thereby reducing their lability and availability.[35–37] However, further research into the effect of speciation changes on lability is required to avoid the potential risk of future remobilisation. During the management and remediation of contaminated sites, it is crucial to continually monitor DGT parameters such as C_{DGT}, the R value, and T_c, in conjunction with changes in soil physicochemical properties, to evaluate the true efficacy of remediation measures, rather than relying solely on the reduction of total concentrations. Particular attention should be paid to areas with high R values and low T_c values, as these represent priority targets for remediation. Furthermore, site-specific remediation strategies should be developed based on the distinct characteristics of heavy metal behaviour in different industrial soil types.

3.7 Limitations and future outlook

This study utilised DGT in combination with soil property analysis to provide a deep insight into the kinetic behaviour and controlling mechanisms of As, Cd, and Pb in different industrial soils, yielding several important findings. However, the study has some limitations. Firstly, correlation analysis reveals statistical associations rather than direct causal relationships. Secondly, the behaviour of heavy metals in soil is a complex, multifactorial process, and this study could not account for all potential influencing factors. For instance, the negative correlations observed between Pb_K_d and total Al, Fe, and Mn warrant more in-depth mechanistic investigation. Additionally, a couple of potential factors could have influenced the accuracy of the data: first, the industrial soil itself may exhibit strong absorption on the particle, leading to underestimated DGT measurements; second, slight soil dehydration might have occurred during the experiment due to indoor air conditioning.

Future research should therefore focus on the following areas: (1) employing advanced characterisation techniques (*e.g.*, X-ray absorption fine structure, XAFS) to directly identify the speciation of heavy metals in the soil and their binding mechanisms with Fe, Mn, and Al oxides, and organic matter. This would help quantitatively elucidate how soil properties influence DGT kinetic parameters, particularly to reveal the chemical mechanisms behind the negative correlations observed for

Pb_K_d. (2) Using multivariate statistical analyses or machine learning models to integrate a more comprehensive suite of soil properties (including different forms of organic matter, clay mineralogy, *etc.*) with DGT kinetic parameters. This would help reveal the synergistic effects of interactive factors on heavy metal behaviour. (3) Conducting long-term, *in situ* monitoring with DGT to evaluate the long-term effectiveness of various soil remediation measures under real-world environmental conditions. Simultaneously, linking DGT-measured labile concentrations directly with ecotoxicity test results (*e.g.*, plant uptake and soil fauna toxicity) is essential for establishing robust, DGT-based ecological risk thresholds and predictive models for a more comprehensive risk assessment.

4 Conclusions

This study comprehensively evaluated the contamination status, labile fractions, and solid-phase resupply dynamics of As, Cd, and Pb in soils from various industrial sites, using DGT in conjunction with traditional analytical methods. We also explored the mechanisms by which soil physicochemical properties (pH, SOM, CEC, total Al, total Fe, and total Mn) control the environmental behaviour of these heavy metals.

The research showed that the non-ferrous metal smelting site (*e.g.*, NMS3) was the primary pollution hotspot with the highest total metal concentrations. The DGT-measured parameters (C_{DGT}, R, and T_c) revealed the dynamic and site-specific nature of heavy metal lability. Notably, total As was strongly correlated with the bioavailable fraction (C_{SE}), suggesting its high activity. Total Cd was strongly correlated with multiple DGT parameters, indicating a high degree of association between its various labile forms and a generally high level of activity. In contrast, Pb appeared to exist in both highly labile forms and more stable, less mobile fractions. The kinetic parameter T_c effectively quantified the solid-phase resupply ability and rate. Cd and Pb exhibited high lability and rapid resupply potential at several sites (*e.g.*, NMS3 and SC2/SC3 for Cd; SC3, NMS3, and MPMM1 for Pb). The study identified key controlling mechanisms: a decrease in pH was found to significantly increase the availability of Cd and Pb, whilst Fe–Mn oxides played a dominant role in the immobilisation of Pb and As. CEC primarily influenced the soluble fractions of As and Cd, and SOM had a lower effect on soluble Pb.

By integrating these DGT parameters and soil properties, this study identified several important sites with high potential environmental risk due to high metal lability and/or rapid resupply kinetics, including chemical industry site CI1 (Cd and Pb), coal mining site CM1 (As and Cd), non-ferrous metal smelt site NMS3 (Cd and Pb), and steel coking sites SC2/SC3 (Cd and Pb). The research underscores the unique advantage of the DGT technique for revealing the complex environmental behaviour of heavy metals, providing dynamic information that is crucial for accurate risk assessment and mechanistic understanding. These findings offer a critical scientific basis for developing targeted, lability-based risk management and remediation strategies for contaminated sites, particularly those involving pH regulation and amendments with Fe–Mn materials. Future research should combine this approach with more advanced micro-characterisation techniques and multi-factor interaction analysis to fully elucidate the complex behaviour of heavy metals in heterogeneous soil environments.

Author contributions

YS was involved in conceptualization, methodology, software, validation, formal analysis, investigation, resources, data curation, writing – original draft, and visualization. YL contributed to the methodology, experiments and data curation. QR and LW contributed to experiments and data curation. QG contributed to supervision, funding acquisition, and conceptualization.

Conflicts of interest

The authors declare that they have no known competing financial interests or personal relationships that could have appeared to influence the work reported in this paper.

Data availability

Backup experimental data are available from the corresponding author upon reasonable request. All data generated or analyzed during this study are included in this article.

References

1 Y. Sun, H. Li, G. Guo, K. T. Semple and K. C. Jones, Soil contamination in China: current priorities, defining background levels and standards for heavy metals, *J. Environ. Manage.*, 2019, **251**, 109512.
2 A. Chamannejadian, A. A. Moezzi, G. Sayyad, A. Jahangiri and A. Jafarnejadi, Spatial distribution of lead in calcareous soils and rice seeds of Khuzestan, Iran, *Malays. J. Soil Sci.*, 2011, **15**, 115–125.
3 E. Kobayashi, Y. Okubo, Y. Suwazono, T. Kido, M. Nishijo, H. Nakagawa and K. Nogawa, Association between total cadmium intake calculated from the cadmium concentration in household rice and mortality among inhabitants of the cadmium-polluted Jinzu River basin of Japan, *Toxicol. Lett.*, 2002, **129**, 85–91.
4 H. L. Needleman, A. Schell, D. Bellinger, A. Leviton and E. N. Allred, The long-term effects of exposure to low doses of lead in childhood: an 11-year follow-up report, *N. Engl. J. Med.*, 1990, **322**, 83–88.
5 G. V. Motuzova, T. M. Minkina, E. A. Karpova, N. U. Barsova and S. S. Mandzhieva, Soil contamination with heavy metals as a potential and real risk to the environment, *J. Geochem. Explor.*, 2014, **144**, 241–246.
6 L. Jiang, M. Zhong, L. Zhang, J. Zhang, X. Jia, D. Han, D. Zhang, T. Xia and Y. Yao, Establishing a risk based framework for contaminated site management in China, *Environ. Pollut. Control*, 2014, **36**, 1–10.
7 S. Silver, Frontiers in ecology and the environment, *Bull. Ecol. Soc. Am.*, 2006, **87**, 276–277.

8 J. Luo, X. Wang, H. Zhang and W. Davison, Theory and application of diffusive gradients in thin films soils, *J. Agro-Environ. Sci.*, 2011, **30**, 205–213.
9 R. Chen, T. Gao, N. Cheng, G. Ding, Q. Wang, R. Shi, G. Hu and X. Cai, Application of DGT/DIFS to assess bioavailable Cd to maize and its release in agricultural soils, *J. Hazard. Mater.*, 2021, **411**, 124837.
10 C. Guo, T. Zhang, S. Hou, J. Lv, Y. Zhang, F. Wu, Z. Hua, W. Meng, H. Zhang and J. Xu, Investigation and application of a new passive sampling technique for *in situ* monitoring of illicit drugs in waste waters and rivers, *Environ. Sci. Technol.*, 2017, **51**, 9101–9108.
11 Y. Wang, Y. Su and S. Lu, Predicting accumulation of Cd in rice (*Oryza sativa* L.) and soil threshold concentration of Cd for rice safe production, *Sci. Total Environ.*, 2020, **738**, 139805.
12 S.-W. Li, M.-Y. Li, H.-J. Sun, H.-B. Li and L. Q. Ma, Lead availability in different fractions of mining- and smelting-contaminated soils based on a sequential extraction and mouse kidney model, *Environ. Pollut.*, 2020, **262**, 114253.
13 D. Xu, G. Bo, W. Peng, G. Li, X. Wan and Y. Li, Application of DGT/DIFS and geochemical baseline to assess Cd release risk in reservoir riparian soils, China, *Sci. Total Environ.*, 2019, **646**, 1546–1553.
14 U.S. Environmental Protection Agency, *Test methods for evaluating solid waste, SW-846, method 9081*, Washington DC, 1986.
15 J. Luo, H. Zhang, F.-J. Zhao and W. Davison, Distinguishing Diffusional and Plant Control of Cd and Ni Uptake by Hyperaccumulator and Nonhyperaccumulator Plants, *Environ. Sci. Technol.*, 2010, **44**, 6636–6641.
16 H. Zhang, W. Davison, S. Miller and W. Tych, In situ high resolution measurements of fluxes of Ni, Cu, Fe, and Mn and concentrations of Zn and Cd in porewaters by DGT, *Geochim. Cosmochim. Acta*, 1995, **59**, 4181–4192.
17 H. Zhang and W. Davison, in *Soil and Water Pollution Monitoring, Protection and Remediation*, ed. I. Twardowska, H. E. Allen, M. M. Häggblom and S. Stefaniak, Springer Netherlands, Dordrecht, 2006, vol. 69, pp. 187–197.
18 H. M. Conesa, R. Schulin and B. Nowack, Suitability of using diffusive gradients in thin films (DGT) to study metal availability in mine tailings: possibilities and constraints, *Environ. Sci. Pollut. Res.*, 2010, **17**, 657–664.
19 Y. Sun, G. Guo, H. Shi, M. Liu, A. Keith, H. Li and K. C. Jones, Decadal shifts in soil pH and organic matter differ between land uses in contrasting regions in China, *Sci. Total Environ.*, 2020, **740**, 139904.
20 Y.-R. Huang, S.-S. Liu, J.-X. Zi, S.-M. Cheng, J. Li, G.-G. Ying and C.-E. Chen, In situ insight into the availability and desorption kinetics of per-and polyfluoroalkyl substances in soils with diffusive gradients in thin films, *Environ. Sci. Technol.*, 2023, **57**, 7809–7817.
21 J. Zhang, L. Yang, Y. Liu, M. Xing, Y. Wu and H. Bing, Pollution and mobility of heavy metals in the soils of a typical agricultural zone in eastern China, *Environ. Geochem. Health*, 2024, **46**, 91.
22 F. Degryse, E. Smolders, H. Zhang and W. Davison, Predicting availability of mineral elements to plants with the DGT technique: a review of experimental data and interpretation by modelling, *Environ. Chem.*, 2009, **6**, 198–218.
23 W. Liu, T. Hu, Y. Mao, M. Shi, C. Cheng, J. Zhang, S. Qi, W. Chen and X. Xing, The mechanistic investigation of geochemical fractionation, availability and release kinetic of heavy metals in contaminated soil of a typical copper-smelter, *Environ. Pollut.*, 2022, **306**, 119391.
24 B. J. Alloway, *Heavy Metals in Soils: Trace Metals and Metalloids in Soils and Their Availability*, Springer Science & Business Media, 2012, vol. 22.
25 F. J. Stevenson, *Humus Chemistry: Genesis, Composition, Reactions*, John Wiley & Sons, 1994.
26 P. L. Smedley and D. G. Kinniburgh, A review of the source, behaviour and distribution of arsenic in natural waters, *Appl. Geochem.*, 2002, **17**, 517–568.
27 A. Soenmezay, M. S. Öncel and N. Bektaş, Adsorption of lead and cadmium ions from aqueous solutions using manganoxide minerals, *Trans. Nonferrous Met. Soc. China*, 2012, **22**, 3131–3139.
28 D. L. Sparks, B. Singh and M. G. Siebecker, *Environmental Soil Chemistry*, Elsevier, 2022.
29 M. Hu, Z. Zhang, Y. Zhang, M. Zhan, W. Qu, G. He and Y. Zhou, Development of human dermal PBPK models for the bisphenols BPA, BPS, BPF, and BPAF with parallel-layered skin compartment: basing on dermal administration studies in humans, *Sci. Total Environ.*, 2023, **868**, 161639.
30 D. Xu, B. Gao, W. Peng, L. Gao, X. Wan and Y. Li, Application of DGT/DIFS and geochemical baseline to assess Cd release risk in reservoir riparian soils, China, *Sci. Total Environ.*, 2019, **646**, 1546–1553.
31 P. Srivastava, N. Bolan, V. Casagrande, J. Benjamin, S. A. Adejumo, M. Sabir, Z. U. R. Farooqi and A. Sarkar, in *Appraisal of Metal (Loids) in the Ecosystem*, Elsevier, 2022, pp. 331–360.
32 R. O. Enesi, M. Dyck, S. Chang, M. S. Thilakarathna, X. Fan, S. Strelkov and L. Y. Gorim, Liming remediates soil acidity and improves crop yield and profitability - a meta-analysis, *Front. Agron.*, 2023, **5**, 1194896.
33 L.-L. He, D.-Y. Huang, Q. Zhang, H.-H. Zhu, C. Xu, B. Li and Q.-H. Zhu, Meta-analysis of the effects of liming on soil pH and cadmium accumulation in crops, *Ecotoxicol. Environ. Saf.*, 2021, **223**, 112621.
34 C. Wang, W. Li, Z. Yang, Y. Chen, W. Shao and J. Ji, An invisible soil acidification: critical role of soil carbonate and its impact on heavy metal availability, *Sci. Rep.*, 2015, **5**, 12735.
35 M. V. Ghandali, S. Safarzadeh, R. Ghasemi-Fasaei and S. Zeinali, Heavy metals immobilization and availability in multi-metal contaminated soil under ryegrass cultivation

as affected by ZnO and MnO_2 nanoparticle-modified biochar, *Sci. Rep.*, 2024, **14**, 10684.

36 H. Hu, X. Li, X. Gao, L. Wang, B. Li, F. Zhan, Y. He, L. Qin and X. Liang, A review on the multifaceted effects of δ-MnO_2 on heavy metals, organic matter, and other soil components, *RSC Adv.*, 2024, **14**, 37752–37762.

37 B. P. Von Der Heyden and A. N. Roychoudhury, Application, Chemical Interaction and Fate of Iron Minerals in Polluted Sediment and Soils, *Curr. Pollut. Rep.*, 2015, **1**, 265–279.